Glycobiology, 2021, 1–7
doi: 10.1093/glycob/cwab009
Communication

Microbial Biology

Surface acoustic wave (SAW) real-time interaction analysis of influenza A virus hemagglutinins with sialylated neoglycolipids

Johanna Detzner, Daniel Steil, Gottfried Pohlentz, Nadine Legros and Johannes Müthing[1]

Institute of Hygiene, University of Münster, Robert-Koch-Str. 41, D-48149 Münster, Germany

[1]To whom correspondence should be addressed: Tel: +492518355192; Fax: +492518355341; e-mail: jm@uni-muenster.de

Received 22 July 2020; Revised 14 January 2021; Accepted 14 January 2021

Abstract

Real-time interaction analysis of H1 hemagglutinin from influenza A H1N1 (A/New York/18/2009) and H7 hemagglutinin from influenza A H7N7 (A/Netherlands/219/03) with sialylated neoglycolipids (neoGLs) was performed using the surface acoustic wave (SAW) technology. The produced neoGLs carried phosphatidylethanolamine (PE) as lipid anchor and terminally sialylated lactose (Lc2, Galβ1-4Glc) or neolactotetraose (nLc4, Galβ1-4GlcNAcβ1-3Galβ1-4Glc) harboring an *N*-acetylneuraminic acid (Neu5Ac). Using α2–6-sialylated neoGLs, H1 and H7 exhibited marginal attachment toward II^{6}Neu5Ac-Lc2-PE, whereas *Sambucus nigra* lectin (SNL) exhibited strong binding and *Maackia amurensis* lectin (MAL) was negative in accordance with their known binding preference toward a distal Neu5Acα2–6Gal- and Neu5Acα2–3Gal-residue, respectively. H1 revealed significant binding toward IV^{6}Neu5Ac-nLc4-PE when compared to weak interaction of H7, whereas SNL showed strong and MAL no attachment corresponding to their interaction specificities. Additional controls of MAL and SNL with α2–3-sialylated II^{3}Neu5Ac-Lc2-PE and IV^{3}Neu5Ac-nLc4-PE underscored the reliability of the SAW technology. Pre-exposure of model membranes spiked with α2–6-sialylated neoGLs to *Vibrio cholerae* neuraminidase substantially reduced the binding of the hemagglutinins and the SNL reference. Collectively, the SAW technology is capable of accurate measuring binding features of hemagglutinins toward neoGL-spiked lipid bilayers, which can be easily loaded to the functionalized biosensor gold surface thereby simulating biological membranes and suggesting promising clinical application for influenza virus research.

Key words: H1N1, H7N7, lectins, neuraminic acid, virus binding

Introduction

Influenza (commonly known as "flu") is an infectious respiratory disease and typically characterized by annual seasonal epidemics and sporadic pandemic outbreaks caused by influenza A strains of zoonotic origin (Krammer et al. 2018). Annual epidemics of influenza are estimated to account for ~1 billion infections, 3–5 million cases of severe illness and half million deaths worldwide per year (Krammer et al. 2018). The 2009 influenza A/H1N1 pandemic virus originated in pigs (as "mixing vessels") prior to infecting humans (Shapshak et al. 2011). Infections of poultry and humans with H7 subtypes have increased markedly in the past and mild to fatal infections were caused by zoonotic important H7 subtypes including H7N7 (Abdelwhab et al. 2014).

There are two principal viral surface glycoproteins (outer "spikes"), the hemagglutinin (H) and the neuraminidase (N), which are utilized to categorize and group influenza viruses (Arias et al. 2009). Sialic acid linked to glycoproteins and gangliosides is exploited

by the hemagglutinin of influenza A viruses as a receptor for cell entry and variations in the receptor specificity are important determinants for host range, tissue tropism and transmissibility of these viruses (Liu et al. 2010; Matrosovich et al. 2015). Avian viruses most commonly bind to sialic acid linked α2–3 to galactose, whereas human viruses bind to sialic acid in α2–6 configuration (Matrosovich et al. 1997; Air 2014). However, sialic acid linkage alone is insufficient to establish a correlation between receptor specificity of hemagglutinin and the efficient transmission of influenza A viruses, which goes beyond the sialic acid linkage (Viswanathan et al. 2010).

Based on the fabrication of neoglycolipids (neoGLs) (Feizi 2000), a unique carbohydrate microarray system has been developed based on noncovalent immobilization of neoGLs on nitrocellulose-coated glass slides as a powerful means of discovering oligosaccharide ligands for carbohydrate-binding proteins (Liu et al. 2012; Feizi 2013) and deciphering the meta-glycome (Palma et al. 2014; Li and Feizi 2018). Microarrays endowed with neoGLs have been successfully applied to a number of host-pathogen recognition studies aimed at identification of altered binding specificities of hemagglutinins derived from influenza A viruses (Childs et al. 2009; Liu et al. 2010; Crusat et al. 2013). When compared to natural glycosphingolipids, neoGLs harboring a consistent phosphatidylethanolamine (PE) lipid anchor (Pohlentz and Egge 1994) are advantageous for recognition studies, because an effect of lipid heterogeneity on the recognition process can be excluded (Campanero-Rhodes et al. 2007).

Here we report for the first time on real-time interaction analysis of H1 hemagglutinin from influenza A H1N1 (A/New York/18/2009) and H7 hemagglutinin from influenza A H7N7 (A/Netherlands/219/03) with sialylated neoGLs using surface acoustic wave (SAW) technology. The hemagglutinin binding features were determined in comparison to *Maackia amurensis* lectin (MAL) and *Sambucus nigra* lectin (SNL) with known binding preferences toward gangliosides with distal Neu5Acα2–3Gal- and Neu5Acα2–6Gal-residues, respectively (Johansson et al. 1999).

Results

The consistency of the amino acid sequences of commercial hemagglutinin H1 derived from human influenza A (A/New York/18/2009 (H1N1)) and hemagglutinin H7 derived from human influenza A (A/Netherlands/219/03 (H7N7)) used in this study with those deposited at the National Center of Biotechnology Information (NCBI, Bethesda, MD, USA) is shown in the supplementary data, Schemes 1 and 2, respectively. The sensorgrams of the middle channel 3 of the 5-channel biosensor chip are shown for each hemagglutinin and the control lectins as representative measurements.

Interaction of hemagglutinins and reference lectins with II^{6}Neu5Ac-Lc2-PE

The binding profiles of H1 and H7 and of the standard lectins MAL and SNL toward II^{6}Neu5Ac-Lc2-PE are displayed in Figure 1A in comparison to those obtained by preceding treatment of the lipid layer with *Vibrio cholerae* neuraminidase shown in Figure 1B. The complete series of the 5-channel-measurements is available in the supplementary data, Figure Fig. S1A and B. The fragment ion spectrum obtained from a collision-induced dissociation experiment on II^{6}Neu5Ac-Lc2-PE (Figure 1C) clearly corroborates the proposed structure as illustrated in the fragmentation scheme (Figure 1D). Fragment ions containing the nonreducing end, namely B_1 and B_2 as well as the fragment comprising the ethylamino moiety (K) verify the saccharide sequence Neu5Ac-Gal-reductaminated Glc. Fragment ions harboring the lipid moiety as Y_1, Z_1, Y_0, and Z_0 indicate the sequential loss of Neu5Ac and Gal, whereas T and U correspond to the dihexadecyl PE and phosphatidic acid residues, respectively. The binding profile in Figure 1A exhibited a very weak attachment of both hemagglutinins to II^{6}Neu5Ac-Lc2-PE. In contrast, reference SNL showed an exceptionally strong binding toward II^{6}Neu5Ac-Lc2-PE, whereas the control with MAL was negative. The bond strength of H1 slightly declined by 21% and that of SNL decreased by 48% after neuraminidase pretreatment of α2–6-sialylated Lc2-PE, whereas H7 and MAL showed minimal but irrelevant adhesive changes upon enzyme exposure (Figure 1B). Hence, short-duration enzyme application toward the II^{6}Neu5Ac-Lc2-PE-studded model membrane indicated only a minor effect upon removal of α2–6-linked Neu5Ac at the disaccharide backbone in case of H1, while desialylation considerably reduced the formerly strong attachment of reference SNL.

Interaction of hemagglutinins and reference lectins with IV^{6}Neu5Ac-nLc4-PE

The binding curves of H1 and H7 together with those of MAL and SNL references toward the α2–6-sialylated PE-linked tetrasaccharide together with the binding curves obtained by precedent treatment with *V. cholerae* neuraminidase are shown in Figure 2A and B, respectively. The entire set of the 5-channel-measurements is provided in the supplementary data, Figure Fig. S2A and B. The MS^2 spectrum of the produced IV^{6}Neu5Ac-nLc4-PE (Figure 2C), supported by the explanatory fragmentation scheme (Figure 2D), yielded the Y series ions Y_3, Y_2, Y_1 and Y_0 in combination with fragment T (dihexadecyl phosphatidylethanolamine moiety) demonstrating the sequential loss of Neu5Ac, Gal, GlcNAc, Gal, and reduced Glc, thus approving the monosaccharide sequence. The same holds true for the reductethylaminated oligosaccharide fragment K and the double fragmentations Y_3/K, Y_2/K, Y_1/K and Y_0/K, respectively. The adhesion profile of H1 and H7 (Figure 2A) evidenced sizeable binding of H1 and low binding of H7 toward IV^{6}Neu5Ac-nLc4-PE. Application of SNL resulted in a very strong attachment toward the α2–6-sialylated PE-linked tetrasaccharide and MAL did not bind at all. Importantly, the binding strength of H1 toward IV^{6}Neu5Ac-nLc4-PE was significantly higher than that of H7. The bond strength of H1 and H7 dropped by 68% and 12%, respectively, and that of SNL decreased by 27% after neuraminidase exposure of α2–6-sialylated nLc4-PE as shown in Figure 2B. Hence, short-time neuraminidase exposure of the model membrane suggested a significant interaction of H1 with IV^{6}Neu5Ac-nLc4-PE, whereas H7 was involved to a lesser extent in the interaction with the α2–6-sialylated neoGL carrying a tetrasaccharide core.

Interaction of reference lectins MAL and SNL with II^{3}Neu5Ac-Lc2-PE and IV^{3}Neu5Ac-nLc4-PE

The binding profiles of the standard lectins MAL and SNL toward II^{3}Neu5Ac-Lc2-PE and IV^{3}Neu5Ac-nLc4-PE are displayed in Figures 3 and 4, respectively. The corresponding series of the 5-channel-measurements are available in the supplementary data, Figures Fig. S3 and Fig. S4, respectively. The MS^2 spectra of the produced II^{3}Neu5Ac-Lc2-PE (Figure 3B) and IV^{3}Neu5Ac-nLc4-PE (Figure 4B) and the respective explanatory fragmentation schemes (Figures 3C and 4C), exhibit, except for individual differences in signal intensities, the same fragment ions as already observed for the

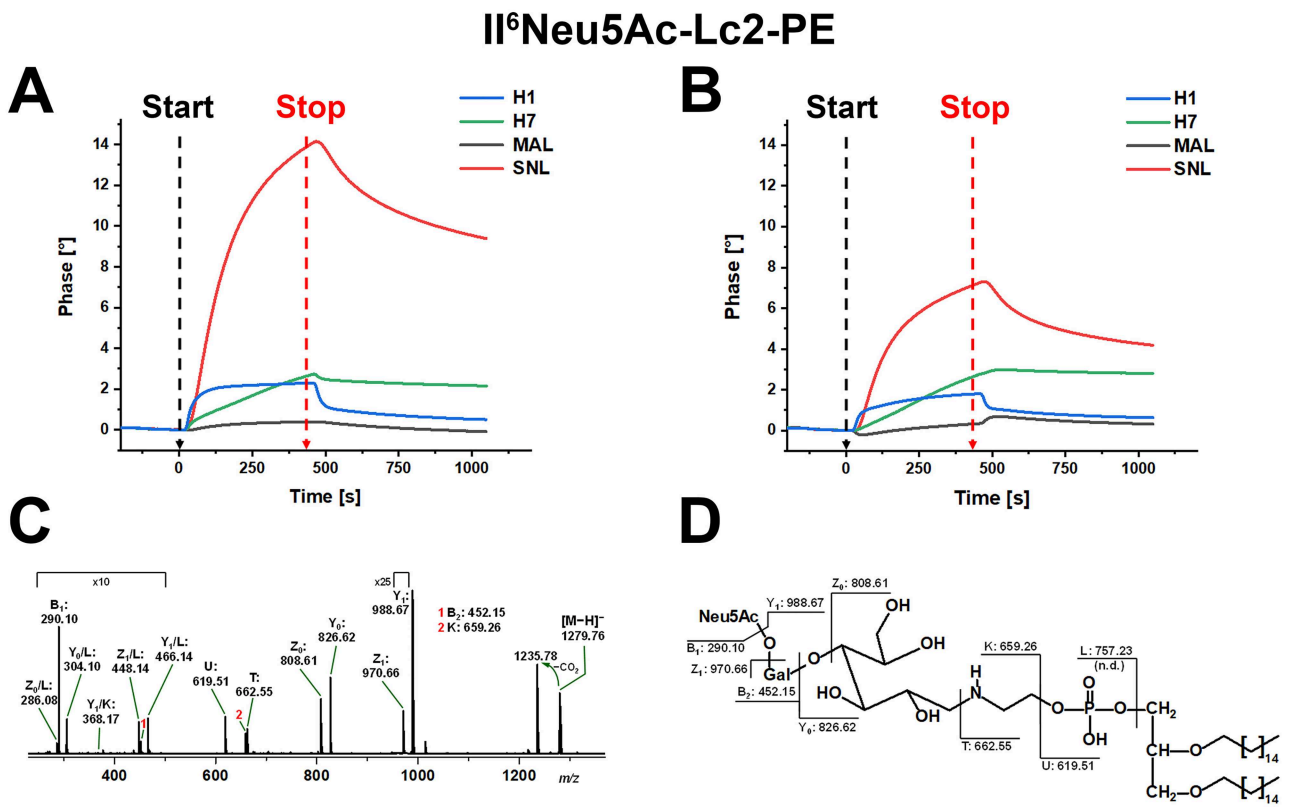

Fig. 1. SAW real-time interaction of influenza A hemagglutinins and standard lectins with II[6]Neu5Ac-Lc2-PE-studded model membranes before (**A**) and after neuraminidase treatment (**B**) as well as MS^2 spectrum (**C**) and fragmentation scheme of II[6]Neu5Ac-Lc2-PE (**D**).

dissociation of II[6]Neu5Ac-Lc2-PE (see Figure 1) and IV[6]Neu5Ac-nLc4-PE (see Figure 2). MAL exhibited a weak but significant positive reaction with α2–3-sialyletd II[3]Neu5Ac-Lc2-PE, while SNL was negative (Figure 3A). The interaction analysis of terminally α2–3-sialylated IV[3]Neu5Ac-nLc4-PE with MAL revealed strong binding, whereas SNL was again negative (Figure 4A). These control experiments underscored the reliability of the SAW technology for unraveling the fine binding characteristics of lectin-carbohydrate interactions.

Conclusion

The SAW technology allows for precise characterization of binding features of lectin-carbohydrate interactions as shown for two hemagglutinins derived from influenza A viruses and two plant lectins that served as controls based on their known binding specificities.

Discussion

The binding specificities of H1 and H7 hemagglutinins derived from human pathogenic influenza A H1N1 (A/New York/18/2009) and influenza A H7N7 (A/Netherlands/219/03), respectively, were evaluated in comparison to MAL and SNL due to their known binding preference toward Neu5Acα2–3Gal- and Neu5Acα2–6Gal-residues, respectively (Johansoon et al. 1999). The employed two α2–6-sialylated neoGLs with Lc2- and nLc4-core allowed for determining a fine characterization regarding specificity in binding and strength in interaction of the viral hemagglutinins H1 and H7 toward short linear receptor candidates. Hemagglutinins and reference lectins were applied in functionally adequate concentrations of 250 nM based on previous experience obtained with bacterial Shiga toxins (Steil et al. 2018). Both hemagglutinins exhibited only irrelevant attachment to II[6]Neu5Ac-Lc2-PE with disaccharide core, whereas the control lectin SNL exhibited strong reaction and MAL no binding at all thereby corroborating the feasibility and reliability of the SAW approach. On the other hand, H1 strongly bound to IV[6]Neu5Ac-nLc4-PE with tetrasaccharide core as well as SNL (whereby the MAL reference was again negative), whereas H7 showed only low binding intensity. However, the utilized short linear receptor portions, i.e. a sialylated di- and tetrasaccharide, are more likely inadequate for a detailed analysis of the H1 and H7 fine specificities, because human virus hemagglutinins bind vastly preferentially to extended glycan receptors with a number of Galβ1-4GlcNAc-repeats beneath the terminal α2–6-sialoside moiety (Miller-Podraza et al. 2000; Matrosovich et al. 2009; Peng et al. 2017). Importantly, it should be mentioned as a cautionary note that a protein label such as polyhistidine tag or biotin can influence specificity of interaction analysis through possible charge effect or spatial hindrance. Thus, future employment of the SAW technology is aimed at analyzing extended receptors, particularly α2–6-linked sialosides, in order to properly contextualize the data. Nevertheless, short-term exposure of the neoGLs II[6]Neu5Ac-Lc2-PE and IV[6]Neu5Ac-nLc4-PE toward *V. cholerae* neuraminidase resulted in abolished binding of control SNL and in case of H1 hemagglutinin to reduced binding to IV[6]Neu5Ac-nLc4-PE, indicating the utility of the SAW approach to recognize enzyme-caused changes of receptor structures. Noteworthy, we used HEPES buffer with a pH-value of 7.5 and performed short-time enzyme exposure of 30 min to exclude any influence of the acetate buffer with pH 5.5 usually

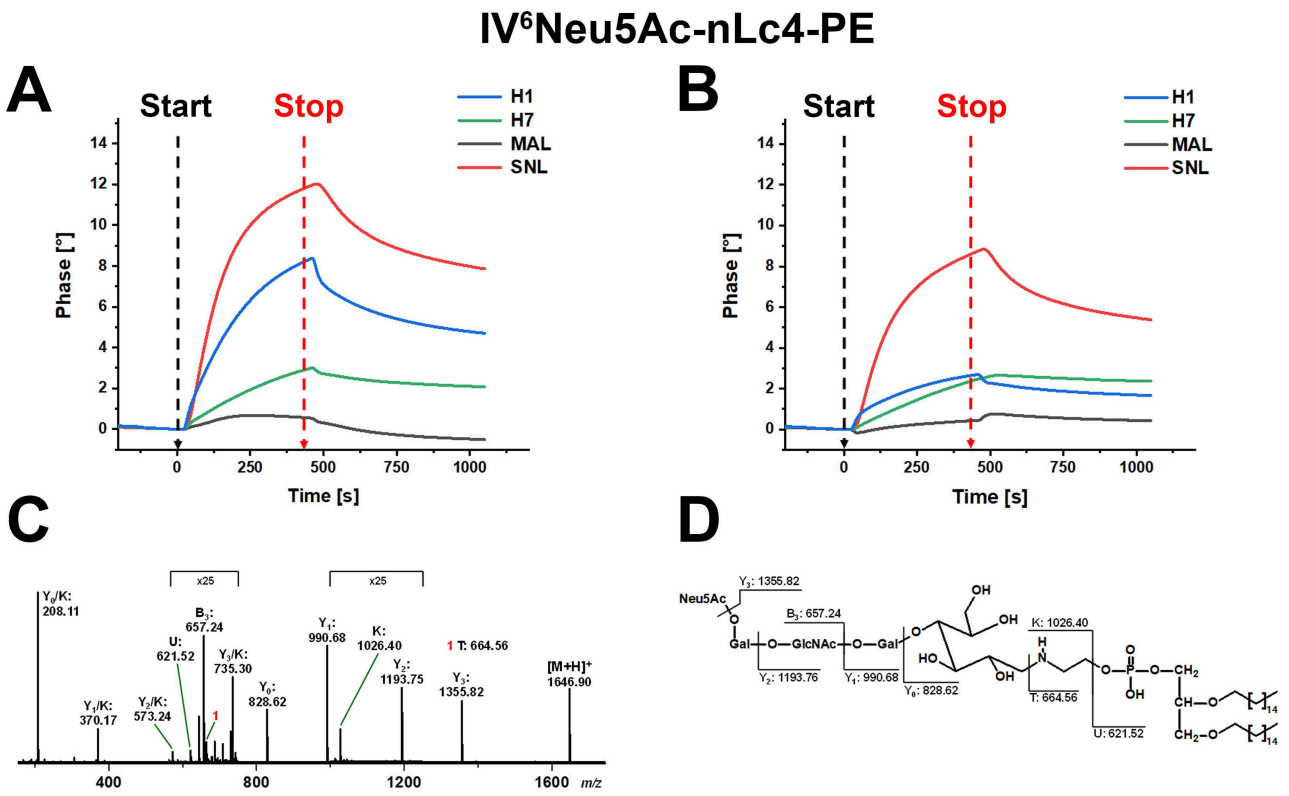

Fig. 2. SAW real-time interaction of influenza A hemagglutinins and standard lectins with IV^{6}Neu5Ac-nLc4-PE-studded model membranes before (**A**) and after neuraminidase treatment (**B**) as well as MS^2 spectrum (**C**) and fragmentation scheme of IV^{6}Neu5Ac-nLc4-PE (**D**).

employed in this enzyme assay. Comparable to our study, well known real-time binding experiments of influenza viruses toward sialylated glycosphingolipids embedded in lipid bilayers have been performed using the quartz crystal microbalance (Sato et al. 1996) or the surface plasmon resonance technology (Hidari et al. 2007). Similarly, the SAW technology is capable of accurately provide real-time readouts measuring binding of compounds involved in biomolecular interaction using gold-coated sensors (Hoß and Bendas 2017). Biomimetic model membranes composed of defined lipids or *lipid raft*-analogous membrane preparations can be easily formulated into vesicles and loaded to the biosensor surfaces (Steil et al. 2018; Detzner et al. 2020). Furthermore, the ability to functionalize commercially available sialoside analogs as neoGLs under relatively simple one-step conditions stands in contrast to comparable technologies such as the surface biolayer interferometry technology requiring far more complex chemistry to adequately functionalize reduced-end sugars typically using streptavidin-coated sensors in conjunction with biotinylated ligands (Carvalho et al. 2017). Overall, the SAW method presented will be appealing using this far more accessible and less labor-intensive method.

Materials and Methods

Glycans and chemicals for synthesis of neoglycolipids (neoGLs)

The sialylated disaccharides 3′-sialyllactose (II^{3}Neu5Ac-Lc2, sodium salt, min 98%; synonym: 3′-SL; Carbosynth Ltd, Compton, UK; cat. OS04397) and 6′-sialyllactose (II^{6}Neu5Ac-Lc2, sodium salt, min 98%; synonym: 6′-SL; Carbosynth Ltd; cat. OS04398) were employed for synthesis of II^{3}Neu5Ac-Lc2-PE and II^{6}Neu5Ac-Lc2-PE, respectively. The compound 1,2-dihexadecyl-*sn*-glycero-3-phosphoethanolamine, ≥99.0% (PE) from Sigma–Aldrich Chemie GmbH (Munich, Germany; cat. 37,161) served as lipid anchor for the synthesis of the neoGLs according to a previously published procedure (Pohlentz and Egge 1994). The sialylated tetrasaccharides 3′-sialyllacto-*N*-neotetraose (IV^{3}Neu5Ac-nLc4, >90%; synonyms: LS-tetrasaccharide d, sialyllacto-*N*-tetraose d; abbr. LST d; Elicityl, Crolles, France; cat. GLY083) and 6′-sialyllacto-*N*-neotetraose (IV^{6}Neu5Ac-nLc4, min 95%; synonyms: LS-tetrasaccharide c, sialyllacto-*N*-tetraose c; abbr. LST c; Carbosynth Ltd, cat. **OL06570**) were used for synthesis of IV^{3}Neu5Ac-nLc4-PE and IV^{6}Neu5Ac-nLc4-PE, respectively. The synthesized neoGLs were denoted following the IUPAC-IUB recommendations (1978). Methanol and chloroform were purchased from Carl Roth GmbH (Karlsruhe, Germany) and were of HPLC grade purity. Dimethylsulfoxide (DMSO) BioReagent (>99.9%) and sodium cyanoborohydride, reagent grade ($NaBH_3CN$) were from Sigma–Aldrich (cat. D8418 and 156159, respectively).

Synthesis of II^{3}Neu5Ac-Lc2-PE and II^{6}Neu5Ac-Lc2-PE

The amount of 111 mg of II^{3}Neu5Ac-Lc2 or II^{6}Neu5Ac-Lc2 was suspended in 500 µL of DMSO, and 3.5 mL of methanol were added. A volume of 13.5 mL of a PE solution adjusted to 10 mg/mL in chloroform/methanol (2/1, v/v) was applied and the mixture was shaken for 2 h at 60°C. Eight 500 µL portions of a newly prepared $NaBH_3CN$ solution (10 mg/mL in chloroform/methanol (1/1, v/v) containing 1% acetic acid) were added one after another over 16 h and the mixture was heated to 60°C. After solvent evaporation

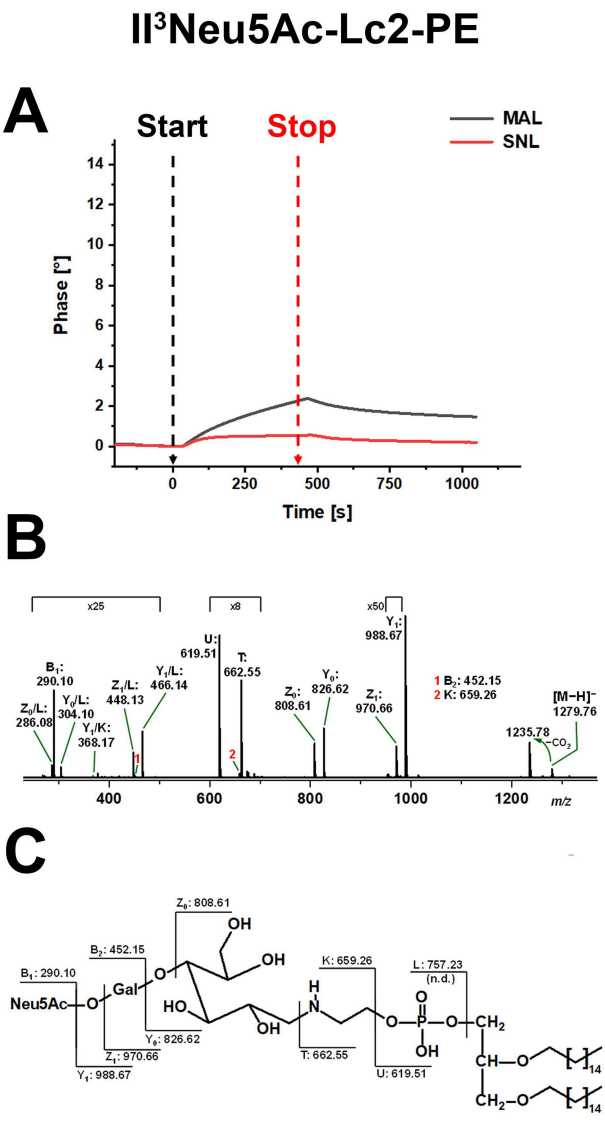

Fig. 3. SAW real-time interaction of MAL and SNL standard lectins with II^{3}Neu5Ac-Lc2-PE-studded model membranes (**A**) together with the MS^2 spectrum (**B**) and fragmentation scheme of II^{3}Neu5Ac-Lc2-PE (**C**).

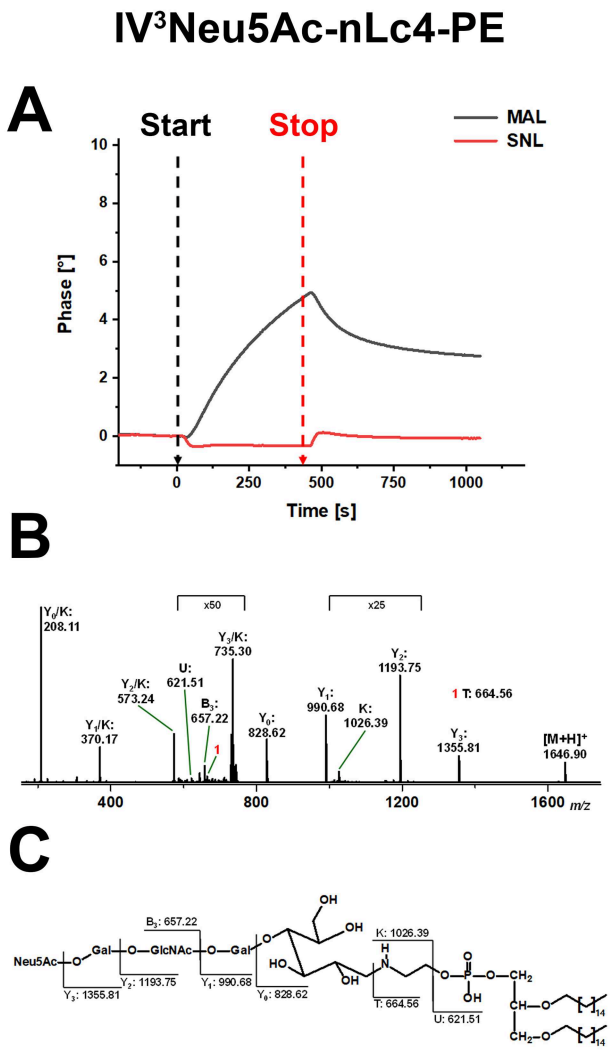

Fig. 4. SAW real-time interaction of MAL and SNL standard lectins with IV^{3}Neu5Ac-nLc4-PE-studded model membranes (**A**) together with the MS^2 spectrum (**B**) and fragmentation scheme of IV^{3}Neu5Ac-nLc4-PE (**C**).

the residue was redissolved in water, dialyzed and freeze-dried. The procedure yielded 212.1 and 217.3 mg of II^{3}Neu5Ac-Lc2-PE and II^{6}Neu5Ac-Lc2-PE, respectively.

Synthesis of IV^{3}Neu5Ac-nLc4-PE and IV^{6}Neu5Ac-nLc4-PE

The amounts of 28 mg of IV^{3}Neu5Ac-nLc4 and 24.5 mg of IV^{6}Neu5Ac-nLc4 were dissolved in 125 µL of DMSO and 875 µL of methanol, mixed with 2.2 and 1.9 mL of a solution of PE [10 mg/mL in chloroform/methanol (2/1, v/v)], respectively. The mixture was then shaken for 2 h at 60°C. Afterwards eight 200 µL portions of a newly prepared $NaBH_3CN$ solution (10 mg/mL in chloroform/methanol (1/1, v/v) containing 1% acetic acid) were added stepwise, followed by keeping the mixtures for a time period of 16 h at 60°C. For completing the conversions, 1.5 mL of the PE solution and five 200 µL aliquots of freshly prepared $NaBH_3CN$ solution were added, and the reaction was allowed to progress for further 16 h at 60°C. The yield after vaporization of the solvent, dialysis and freeze-drying was 42.4 and 39.5 mg of IV^{3}Neu5Ac-nLc4-PE and IV^{6}Neu5Ac-nLc4-PE, respectively.

Mass spectrometry

The produced neoGLs were taken up in chloroform/methanol (2/8, v/v). Electrospray-ionization MS analysis was performed using a SYNAPT G2-S mass spectrometer (Waters, Manchester, UK) endowed with a Z-spray source. Neu5Ac-Lc2-PE and Neu5Ac-nLc4-PE species were analyzed in the negative ion and positive ion sensitivity mode, respectively (Steil et al. 2015; Pohlentz et al. 2019).

Preparation of vesicles employed as model membranes

Small unilamellar vesicles were prepared with 1,2-dioleoyl-*sn*-glycero-3-phosphatidylcholine (DOPC; Sigma–Aldrich, Steinheim, Germany; cat. P6354), cholesterol (Sigma–Aldrich; cat. C8667), sphingomyelin derived from calf brain (Steil et al. 2018), and

the produced neoGLs II^{3}Neu5Ac-Lc2-PE, II^{6}Neu5Ac-Lc2-PE, IV^{3}Neu5Ac-nLc4-PE, or IV^{6}Neu5Ac-nLc4-PE (see above). Vesicles were composed of the matrix lipids DOPC, sphingomyelin, cholesterol and the respective neoGL in a 6:1:2:1 ratio (each by weight) as recently described (Steil et al. 2018; Detzner et al. 2020).

SAW real-time interaction analysis

Label-free measurement was performed using the SAM® 5 blue surface acoustic wave (SAW) instrument (SAW Instruments GmbH, Bonn, Germany) equipped with a 5-channel configuration as previously described (Steil et al. 2018; Detzner et al. 2020). Briefly, the gold surface of the biosensor chips was functionalized with 11-mercaptoundecanoic acid. After loading of the chips with the model membranes, hemagglutinins and standard lectins were applied with concentrations of 250 nM in HEPES buffer (pH 7.5) supplemented with 0.1 mM $CaCl_2$. Changes in the phase shift φ were monitored online (Steil et al. 2018; Detzner et al. 2020). In case of precedent neuraminidase treatment, the model membrane was exposed for 30 min before the adhesion assay to *V. cholera*e neuraminidase (Sigma–Aldrich; cat. N7885; EC 3.2.1.18) in HEPES buffer supplemented with 9 mM $CaCl_2$ using an enzyme concentration of 5 mU/mL.

Influenza hemagglutinins and standard lectins

The H1 hemagglutinin from influenza A H1N1 (A/New York/18/2009) (cat. 40009-V08B-50, NCBI accession ACR08536.1) and the H7 hemagglutinin from influenza A H7N7 (A/Netherlands/219/03) (cat. 11082-V08B-50, NCBI accession AAR02640.2), both expressed with a polyhistidine tag (10xHis) at the C-terminus, were from Sino Biological (Wayne, PA, USA). The amino acid sequences of the commercial H1 and H7 were identical to those of H1 from influenza A H1N1 (A/New York/18/2009) (Garten et al. 2009) and H7 from influenza A H7N7 (A/Netherlands/219/03) (Fouchier et al. 2004) deposited at the NCBI (https://www.ncbi.nlm.nih.gov/protein/ACR08536.1 and https://www.ncbi.nlm.nih.gov/protein/AAR02640.2, respectively) as shown in the supplementary data, Schemes 1 and 2, respectively. Employed standard lectins, both from Vector Laboratories, Inc. (Burlingame, CA, USA), were MAL (biotinylated MAL II, cat. B-1265) and SNL (biotinylated SNL, cat. B-1305).

Supplementary data

Supplementary data for this article are available online at http://glycob.oxfordjournals.org/.

Acknowledgments

This article is dedicated to the memory of Prof. Dr. Elizabeth Hounsell, Emeritus Professor of Biological Chemistry at Birkbeck College London, who passed away on 21 February 2020 after a long and serious illness. Liz was a pioneer in the development and application of modern analytical techniques to structure determination of biologically important glycoconjugates. We lost an outstanding scientist and a very dear friend. She will be greatly missed and we will always keep her in honorable memory. The expert technical assistance of Dagmar Mense and Nikola Skutta is gratefully acknowledged.

Funding

German Research Foundation (Deutsche Forschungsgemeinschaft, DFG), grant number MU845/7-1 with reference number 404813761 (J.M.) and the German Federal Ministry of Education and Research (BMBF) with assistance of InfectControl 2020 (TFP-TV8-AS12, ref. no. 03ZZ0802H) and InfectControl 2020 IRMRESS (ref. no. 03ZZ0805B).

Conflict of interest statement

None declared.

Abbreviations

H, hemagglutinin ; Lc2, lactose, Galβ1-4Glc ; MAL, *Maackia amurensis* lectin ; MS, mass spectrometry ; neoGL(s), neoglycolipid(s) ; Neu5Ac, *N*-acetylneuraminic acid ; nLc4, neolactotetraose, Galβ1-4GlcNAcβ1-3Galβ1-4Glc ; PE, phosphatidylethanolamine ; SAW, surface acoustic wave ; SNL, *Sambucus nigra* lectin.

References

Abdelwhab EM, Veits J, Mettenleiter TC. 2014. Prevalence and control of H7 avian influenza viruses in birds and humans. *Epidemiol Infect*. 142:896–920.

Air GM. 2014. Influenza virus-glycan interaction. *Curr Opin Virol*. 7:128–133.

Arias CF, Escalera-Zamudio M, de Los Dolores Soto-Del Rio M, Cobián-Güemes AG, Isa P, López S. 2009. Molecular anatomy of 2009 influenza virus A (H1N1). *Arch Med Res* 40:643–654.

Campanero-Rhodes MA, Smith A, Chai W, Sonnino S, Mauri L, Childs RA, Zhang Y, Ewers H, Helenius A, Imberty A *et al.* 2007. *N*-glycolyl GM1 ganglioside as a receptor for simian virus 40. *J Virol*. 81:12846–12858.

Carvalho SB, Moleirinho MG, Wheatley D, Welsh J, Gantier R, Alves PM, Peixoto C, Carrondo MJ. 2017. Universal label-free in-process quantification of influenza virus-like particles. *Biotechnol J*. 12:1700031.

Childs RA, Palma AS, Wharton S, Matrosovich T, Liu Y, Chai W, Campanero-Rhodes M, Zhang Y, Eickmann M, Kiso M *et al.* 2009. Receptor-binding specificity of pandemic influenza A (H1N1) 2009 virus determined by carbohydrate microarray. *Nat Biotechnol*. 27:797–799.

Crusat M, Liu J, Palma AS, Child RA, Liu Y, Wharton SA, Lin YP, Coombs PJ, Martin SR, Matrosovich M *et al.* 2013. Changes in the hemagglutinin of H5N1 viruses during human infection – Influence on receptor binding. *Virology*. 447:326–337.

Detzner J, Steil D, Pohlentz G, Legros N, Humpf HU, Mellmann A, Karch H, Müthing J. 2020. Real-time interaction analysis of Shiga toxins and membrane microdomains of primary human brain microvascular endothelial cells. *Glycobiology*. 30:174–185.

Feizi T. 2000. Carbohydrate-mediated recognition sytsems in innate immunity. *Immunol Rev*. 173:79–88.

Feizi T. 2013. Carbohydrate recognition in the immune system: Contributions of neoglycolipid-based microarrays to carbohydrate ligand discovery. *Ann N Y Acad Sci*. 1292:33–44.

Fouchier RA, Schneeberger PM, Rozendaal FW, Broekman JM, Kemink SA, Munster V, Kuiken T, Rimmelzwaan GF, Schutten M, van Doornum GJ *et al.* 2004. Avian influenza A virus (H7N7) associated with human conjunctivitis and a fatal case of acute respiratory distress syndrome. *Proc Natl Acad Sci USA*. 101:1356–1361.

Garten RJ, Davis CT, Russell CA, Shu B, Lindstrom S, Balish A, Sessions WM, Xu X, Skepner E, Deyde V *et al.* 2009. Antigenic and genetic characteristics of swine-origin 2009 A(H1N1) influenza viruses circulating in humans. *Science*. 325:197–201.

Hidari KI, Shimada S, Suzuki Y, Suzuki T. 2007. Binding kinetics of influenza viruses to sialic acid-containing carbohydrates. *Glycoconj J*. 24:583–590.

Hoß SG, Bendas G. 2017. Mass-sensitive biosensor systems to determine the membrane interaction of analytes. *Methods Mol Biol*. 1520:145–157.

IUPAC-IUB Commission on Biochemical Nomenclature. 1978. The nomenclature of lipids (recommendations 1976). *J Lipid Res*. 19:114–128.

Johansson L, Johansson P, Miller-Podraza H. 1999. Detection by the lectins from *Maackia amurensis* and *Sambucus nigra* of 3- and 6-linked sialic acid in gangliosides with neolacto chains separated on thin-layer chromatograms and blotted to PVDF membranes. *Anal Biochem*. 267:239–241.

Krammer F, Smith GJD, Fouchier RAM, Peiris M, Kedzierska K, Doherty PC, Palese P, Shaw ML, Treanor J, Webster RG *et al*. 2018. Influenza. *Nat Rev Dis Primers*. 4:3.

Li F, Feizi T. 2018. The neoglycolipid (NGL) technology-based microarrays and future prospects. *FEBS Lett*. 592:3976–3991.

Liu Y, Childs RA, Matrosovich T, Wharton S, Palma AS, Chai W, Daniels R, Gregory V, Uhlendorff J, Kiso M *et al*. 2010. Altered receptor specificity and cell tropism of D222G hemagglutinin mutants isolated from fatal cases of pandemic A (H1N1) 2009 influenza virus. *J Virol*. 84:12069–12074.

Liu Y, Childs RA, Palma AS, Companero-Rhodes MA, Stoll MS, Chai W, Feizi T. 2012. Neoglycolipid-based oligosaccharide microarray system: Preparation of NGLs and their noncovalent immobilization on nitrocellulose-coated glass slides for microarray analyses. *Methods Mol Biol*. 808:117–136.

Matrosovich MN, Gambaryan AS, Teneberg S, Piskarev VE, Yamnikova SS, Lvov DK, Robertson JS, Karlsson KA. 1997. Avian influenza A viruses differ from human viruses by recognition of sialyloligosaccharides and gangliosides and by a higher conservation of the HA receptor-binding site. *J Virol*. 233:224–234.

Matrosovich M, Stech J, Klenk D. 2009. Influenza receptors, polymerase and host range. *Rev Sci Tech*. 28:203–217.

Matrosovich M, Herrler G, Klenk HD. 2015. Sialic acid receptors of viruses. *Top Curr Chem*. 367:1–28.

Miller-Podraza H, Johansson L, Johansson P, Larsson T, Matrosovich M, Karlsson KA. 2000. A strain of human influenza A virus binds to extended but not short gangliosides as assayed by thin-layer chromatography overlay. *Glycobiology*. 10:975–982.

Palma AS, Feizi T, Childs RA, Chai W, Liu Y. 2014. The neoglycolipid (NGL)-based oligosaccharide microarray system poised to decipher the meta-glycome. *Curr Opin Chem Biol*. 18:87–94.

Peng W, de Vries RP, Grant OC, Thompson AJ, McBride R, Tsogtbaatar B, Lee PS, Razi N, Wilson IA, Woods RJ *et al*. 2017. Recent H3N2 viruses have evolved specificity for extended, branched human-type receptors, conferring potential for increased avidity. *Cell Host Microbe*. 21:23–34.

Pohlentz G, Egge H. 1994. Neoglycolipids of 1-deoxy-1-phosphatidylethanolaminolactitol type: Synthesis, structure analysis, and use as probes for characterization of glycosyltransferases. *Methods Enzymol*. 242:127–145.

Pohlentz G, Steil D, Rubin D, Mellmann A, Karch H, Müthing J. 2019. Pectin-derived neoglycolipids: Tools for differentiation of Shiga toxin subtypes and inhibitors of Shiga toxin-mediated cellular injury. *Carbohydr Polym*. 212:323–333.

Sato T, Serizawa T, Okahata Y. 1996. Binding of influenza A virus to monosialoganglioside (GM3) reconstituted in glucosylceramide and sphingomyelin membranes. *Biochim Biophys Acta*. 1285:14–20.

Shapshak P, Chiappelli F, Somboonwitt C, Sinnott J. 2011. The influenza pandemic of 2009: Lessons and implications. *Mol Diagn Ther*. 15: 63–81.

Steil D, Schepers CL, Pohlentz G, Legros N, Runde J, Humpf HU, Karch H, Müthing J. 2015. Shiga toxin glycosphingolipid receptors of Vero-B4 kidney epithelial cells and their membrane microdomain lipid environment. *J Lipid Res*. 56:2322–2336.

Steil D, Pohlentz G, Legros N, Mormann M, Mellmann A, Karch H, Müthing J. 2018. Combining mass spectrometry, surface acoustic wave interaction analysis, and cell viability assays for characterization of Shiga toxin subtypes of pathogenic *Escherichia coli* bacteria. *Anal Chem*. 90: 8989–8997.

Viswanathan K, Chandrasekaran A, Srinivasan A, Raman R, Sasisekharan V, Sasisekharan R. 2010. Glycans as receptors for influenza pathogenesis. *Glycoconj J*. 27:561–570.